



Available online at [www.sciencedirect.com](http://www.sciencedirect.com)


**ScienceDirect**  
 Journal of Hydrodynamics

2015,27(3):321-331

DOI: 10.1016/S1001-6058(15)60489-9



[www.sciencedirect.com/  
 science/journal/10016058](http://www.sciencedirect.com/science/journal/10016058)



## Homotopy-based analytical approximation to nonlinear short-crested waves in a fluid of finite depth\*

WANG Ping (王苹)<sup>1,2</sup>, LU Dong-qiang (卢东强)<sup>1,3</sup>

1. Shanghai Institute of Applied Mathematics and Mechanics, Shanghai University, Shanghai 200072, China

2. School of Mathematics and Physics, Qingdao University of Science and Technology, Qingdao 266061, China

E-mail: [pingwang2003@126.com](mailto:pingwang2003@126.com)

3. Shanghai Key Laboratory of Mechanics in Energy Engineering, Shanghai University, Shanghai 200072, China

(Received January 8, 2014, Revised May 18, 2015)

**Abstract:** A nonlinear short-crested wave system, consisting of two progressive waves propagating at an oblique angle to each other in a fluid of finite depth, is investigated by means of an analytical approach named the homotopy analysis method (HAM). Highly convergent series solutions are explicitly derived for the velocity potential and the surface wave elevation. We find that, at every value of water depth, there is little difference between the kinetic energy and the potential energy for nonlinear waves. The nonlinear short-crested waves with a larger angle of incidence always contain the more potential wave energy. With the aid of the HAM, we obtain the dispersion relation for nonlinear short-crested waves. Furthermore, it is shown that the wave elevation tends to be smoothed at the crest and be sharpened at the trough as the water depth increases, and the wave pressure crests and troughs become steeper with increasing incident wave steepness.

**Key words:** nonlinear short-crested waves, finite water depth, homotopy analysis method (HAM), wave energy, wave profile

### Introduction

A short-crested wave system, made of two progressive wave trains propagating at an angle to each other, occurs in some realistic coastal regions, such as in front of a vertical seawall or an offshore platform where the oblique wave reflection appears, behind an obstacle of finite width where diffracted waves intersect, and on the ocean surface where two swell waves cross with each other. The main motivation for this topic is to study how to design some coastal structures safely. One of the important problems concerned in this field appears to be an accurate prediction of the characteristics of short-crested waves in a fluid of finite

te depth.

For a short-crested wave system, considerable work has been done since the first theoretical model proposed by Fuchs<sup>[1]</sup> in 1952. However, the previous researches on the short-crested waves are mainly within the scope of linear theory which is only valid for the small-amplitude waves. Such models are not appropriate to describe nonlinear short-crested waves of arbitrary amplitude. Furthermore, due to the limitation of mathematical tools, most analytical studies on the nonlinear short-crested wave often follow the well-known perturbation methods which can be applied to weakly nonlinear problems only. For example, Fuchs<sup>[1]</sup> derived a second-order solution in dimensional form by means of a perturbation parameter related to the ratio of the wave height to the wavelength parallel to the wall. Subsequently, Chappellear<sup>[2]</sup> further extended the pioneering work of Fuchs<sup>[1]</sup> to the third-order perturbation approximation.

However, the solutions of Fuchs<sup>[1]</sup> and Chappellear<sup>[2]</sup> were not applicable for the limiting condition of the short-crested waves, i.e., the progressive and standing waves. In 1979 Hsu et al.<sup>[3]</sup> optimized the previous analytical method, in the frame of perturbation

\* Project Supported by the National Key Basic Research Development Program of China (973 Program, Grant No. 2014CB046203), the National Natural Science Foundation of China (Grant No. 11472166) and the Natural Science Foundation of Shanghai (Grant No. 14ZR1416200).

**Biography:** WANG Ping (1975-), Female, Ph. D. Candidate

**Corresponding author:** LU Dong-qiang,

E-mail: [dqlu@shu.edu.cn](mailto:dqlu@shu.edu.cn)

technology, by introducing the wave steepness as the small perturbation parameter, and derived the third-order solution in non-dimensional form, including progressive and standing waves limits. Following the framework of Hsu et al.<sup>[3]</sup>, Roberts<sup>[4]</sup> obtained the third-order expansion based on a three-dimensional generalization of the mapping from the velocity-potential-stream function space to the physical space, and Fenton<sup>[5]</sup> further studied the wave forces and pressures on a vertical wall due to short-crested waves. Recently, Jian et al.<sup>[6]</sup> investigated the short-crested capillary-gravity wave patterns with a uniform current and obtained the third-order approximate solution through a perturbation expanding technique.

Numerical perturbation approximations have been widely applied to the nonlinear short-crested wave system in recent years. Among these, Roberts<sup>[7]</sup> investigated the highly nonlinear properties of steadily propagating short-crested waves in deep water. The 27th order perturbation expansion in terms of the wave steepness was derived numerically. Then the effects of several parameters including the water depth and the incident angle on the wave energy were studied in detail.

In the present study, we will apply the homotopy analysis method (HAM) developed by Liao<sup>[8]</sup> in 1992, which has been demonstrated as a powerful analytical approach for weakly/highly nonlinear problems, in order to investigate analytically nonlinear short-crested waves in a fluid of finite depth. The convergent series solutions for the velocity potential and the surface wave elevation are obtained by introducing a convergence control parameter  $c_0$ . It is found that the nonlinear short-crested wave energy is greatly affected by the oblique angle of incidence. Furthermore, the effect of the water depth on the wave energy and the wave elevation is studied in detail. All the results obtained will help enrich our basic understanding on the characteristics of nonlinear short-crested waves in a fluid of finite depth.

**1. Mathematical formulation**

A system of nonlinear short-crested waves in front of a vertical seawall in a fluid of finite depth  $d$  is considered. Cartesian coordinates  $(x, y, z)$  are taken in such a way that the  $x$ - and  $y$ -axes are fixed on the undisturbed surface while the  $z$ -axis points vertically upwards. The vertical wall coincides with  $y = 0$ . Assuming that the fluid is inviscid and incompressible, and the flow is irrotational, there exists a velocity potential  $\phi(x, y, z, t)$  which satisfies the Laplace equation

$$\nabla^2 \phi = 0, \quad -d \leq z \leq \zeta(x, y, t) \tag{1}$$

where  $\zeta(x, y, t)$  is the surface wave elevation and  $t$  the time variable. The bottom boundary condition reads

$$\left. \frac{\partial \phi}{\partial z} \right|_{z=-d} = 0 \tag{2}$$

In addition, at the wall boundary it holds that

$$\left. \frac{\partial \phi}{\partial y} \right|_{y=0} = 0 \tag{3}$$

The nonlinear kinematic condition is modeled as

$$\frac{\partial \zeta}{\partial t} + \frac{\partial \phi}{\partial x} \frac{\partial \zeta}{\partial x} + \frac{\partial \phi}{\partial y} \frac{\partial \zeta}{\partial y} - \frac{\partial \phi}{\partial z} = 0, \quad z = \zeta(x, y, t) \tag{4}$$

The nonlinear dynamic boundary condition is<sup>[9]</sup>

$$\frac{\partial \phi}{\partial t} + \frac{1}{2} |\nabla \phi|^2 + g\zeta + E = 0, \quad z = \zeta(x, y, t) \tag{5}$$

where  $g$  is the gravitational acceleration and  $E$  is a Bernoulli constant.

There was some confusion regarding whether or not the Bernoulli constant is included in the dynamic boundary condition of periodic traveling waves in the literature. Recently, Vasan and Deconinck<sup>[9]</sup> showed that the two boundary conditions (namely  $E = 0$  or  $E \neq 0$ ) were equivalent up to the addition of a uniform horizontal velocity. In other words, eliminating the Bernoulli constant corresponds to changing the speed of the traveling wave. To make a comparison between the solution obtained by Hsu et al.<sup>[3]</sup> and the third-order series solutions presented here, we also assume  $E = 0$  as made in Ref.[3].

Following Hsu et al.<sup>[3]</sup>, we put all equations into dimensionless form to simplify the formulation. Let  $\varepsilon = ka$ , where  $k$  and  $a$  are the wave number and the amplitude of short-crested waves of the first order, respectively. Then the following dimensionless quantities are adopted

$$x^* = kx, \quad y^* = ky, \quad z^* = kz, \quad t^* = t(gk)^{1/2}, \quad d^* = kd,$$

$$\phi^*(x^*, y^*, z^*, t^*) = \frac{k^2 \phi(x, y, z, t)}{\varepsilon (gk)^{1/2}},$$

$$\zeta^*(x^*, y^*, t^*) = \frac{k\zeta(x, y, t)}{\varepsilon}, \quad \omega^* = \frac{\omega}{(gk)^{1/2}} \tag{6}$$

where  $\omega$  is the angular frequency of the incident or

reflected waves.

Here we consider a system of nonlinear short-crested waves which are formed by two progressive waves propagating at an oblique angle to each other. Let  $\theta$  be the angle of incidence measured from the normal to the wall. Based on the traveling-wave method, we introduce the following independent variable transformations

$$X^* = x^* \sin \theta - \omega^* t^*, \quad Y = y^* \cos \theta, \quad Z^* = z^* \quad (7)$$

Then, we can express the potential function  $\phi^*(x^*, y^*, z^*, t^*) = \phi^*(X^*, Y^*, Z^*)$  and the traveling wave profile  $\zeta^*(x^*, y^*, t^*) = \zeta^*(X^*, Y^*)$ . Thus the short-crested waves can be considered in the coordinates  $(X^*, Y^*, Z^*)$ . With the transformation (7) and dimensionless quantities (6), the governing Eq.(1) and boundary conditions (2)-(3) and (5) are transformed into

$$\frac{\partial^2 \phi}{\partial X^2} \sin^2 \theta + \frac{\partial^2 \phi}{\partial Y^2} \cos^2 \theta + \frac{\partial^2 \phi}{\partial Z^2} = 0 \quad (-d \leq Z \leq \varepsilon \zeta) \quad (8)$$

$$\left. \frac{\partial \phi}{\partial Z} \right|_{Z=-d} = 0 \quad (9)$$

$$\left. \frac{\partial \phi}{\partial Y} \right|_{Y=0} = 0 \quad (10)$$

$$-\omega \frac{\partial \phi}{\partial X} + \varepsilon f + \zeta = 0 \quad (Z = \varepsilon \zeta) \quad (11)$$

where

$$f = \frac{1}{2} \left[ \left( \frac{\partial \phi}{\partial X} \sin \theta \right)^2 + \left( \frac{\partial \phi}{\partial Y} \cos \theta \right)^2 + \left( \frac{\partial \phi}{\partial Z} \right)^2 \right]$$

With Eqs.(7) and (6), we give a combination of Eqs.(4) and (5) on  $Z = \varepsilon \zeta$

$$-\omega^2 \frac{\partial^2 \phi}{\partial X^2} - \frac{\partial \phi}{\partial Z} + \varepsilon \omega \frac{\partial f}{\partial X} + \varepsilon \frac{\partial \phi}{\partial X} \left( \omega \frac{\partial^2 \phi}{\partial X^2} - \varepsilon \frac{\partial f}{\partial X} \right) \cdot \sin^2 \theta + \varepsilon \frac{\partial \phi}{\partial Y} \left( \omega \frac{\partial^2 \phi}{\partial X \partial Y} - \varepsilon \frac{\partial f}{\partial Y} \right) \cos^2 \theta = 0 \quad (12)$$

So the unknown  $\phi$  and  $\zeta$  are governed by Eqs.(8)-(12).

In accordance with Roberts<sup>[7]</sup>, we also quote two quantities which measure how much energy there is in

the waves. Similarly, let  $K_E$  and  $P_E$  be dimensionless mean kinetic and potential energy densities per unit area in the  $(X, Y)$ -plane, respectively, which can be written as

$$K_E = \frac{\omega}{8\pi^2} \int_0^{2\pi} \int_0^{2\pi} \zeta \left( \frac{\partial \phi}{\partial X} + \frac{\partial \zeta}{\partial X} \frac{\partial \phi}{\partial Y} \right) dX dY \quad (13)$$

$$P_E = \frac{1}{8\pi^2} \int_0^{2\pi} \int_0^{2\pi} \zeta^2 dX dY \quad (14)$$

The pressure in the wave motion is given by Bernoulli's theorem in terms of dimensionless quantities as

$$p^* = -\zeta + \varepsilon \omega \frac{\partial \phi}{\partial X} - \varepsilon^2 f \quad (15)$$

where  $p^* = p/(\rho g/k)$ . The dimensionless pressure will be written without the asterisk for convenience throughout the rest of the paper.

## 2. Analytical approach based on the HAM

As is well known, the perturbation methods have been widely applied to solve nonlinear water wave problems. Unfortunately, the perturbation methods depend extremely on the small/large physical parameters in general, and then are valid only for weakly nonlinear problems. To solve the weakly/fully nonlinear problems effectively and accurately, Liao<sup>[8]</sup> proposed the HAM based on the concept of homotopy in algebraic topology. In recent years, the HAM has been applied to many highly nonlinear problems in science, finance and hydrodynamics<sup>[10-21]</sup>. In this section, the HAM is employed to solve the nonlinear partial differential equations (PDEs) (8)-(12) for two unknown variables  $\phi$  and  $\zeta$ .

### 2.1 Solution formulas and initial guesses

Under the assumption that the short-crested waves are propagating without a change of shape, we consider that the wave profile  $\zeta$  is periodic in  $X$  and  $Y$ <sup>[7]</sup>. From physical point of view, it is clear that the wave profile can be expressed as

$$\zeta = \sum_{i,j=0}^{\infty} \beta_{i,j} \cos(iX) \cos(jY) \quad (16)$$

where  $\beta_{i,j}$  is a constant to be determined. According to the governing Eq.(8), the boundary conditions (9) and (10),  $\phi$  should be in the form

$$\phi = \sum_{i,j=0}^{\infty} \alpha_{i,j} \sin(iX) \cos(jY) \cdot \cosh[\sqrt{i^2 \sin^2 \theta + j^2 \cos^2 \theta}(Z + d)] \tag{17}$$

where  $\alpha_{i,j}$  is a constant to be determined. Equations (16) and (17) are called the solution expressions of  $\zeta$  and  $\phi$  respectively, which play important roles in the frame of the HAM. We construct the initial guess for the potential function as

$$\phi_0 = \frac{A}{\sinh d} \sin X \cos Y \cosh(Z + d) \tag{18}$$

where  $A$  is an unknown coefficient. We choose  $\zeta_0 = 0$  as the initial guess for  $\zeta$  to simplify the subsequent solution procedure<sup>[20,21]</sup>. It should be emphasized that the high-order terms can sufficiently provide the corrections for the analytical series solutions due to the nonlinearity inherence in Eqs.(11) and (12) although the initial guess  $\zeta_0$  is zero.

2.2 Continuous variation

The nonlinear boundary-value problem governed by the PDEs (8)-(12) is solved by means of the HAM. Instead of solving these nonlinear PDEs directly, we construct two homotopies  $\Phi$  and  $\eta$ . The homotopy  $\Phi$  satisfies the Laplace equation

$$\frac{\partial^2 \Phi}{\partial X^2} \sin^2 \theta + \frac{\partial^2 \Phi}{\partial Y^2} \cos^2 \theta + \frac{\partial^2 \Phi}{\partial Z^2} = 0$$

and the boundary conditions

$$\frac{\partial \Phi}{\partial Z} \Big|_{Z=-d} = 0, \quad \frac{\partial \Phi}{\partial Y} \Big|_{Y=0} = 0$$

The homotopies  $\Phi$  and  $\eta$  are governed by a new PDES, namely the so-called zeroth-order deformation equations

$$(1 - q)L_1[\Phi - \phi_0] = qc_0 N_1[\Phi] \quad (Z = \varepsilon \eta) \tag{19}$$

$$(1 - q)(\eta - \zeta_0) = qc_0 N_2[\eta, \Phi] \quad (Z = \varepsilon \eta) \tag{20}$$

where  $q \in [0, 1]$  is an embedding parameter,  $c_0$  denotes a nonzero convergence-control parameter,  $L_1[\cdot]$  is an auxiliary linear operator with the property  $L_1[0] = 0$ ,  $N_1[\cdot]$  and  $N_2[\cdot]$  are two nonlinear differential operators defined by

$$N_1[\Phi] = \omega^2 \frac{\partial^2 \Phi}{\partial X^2} + \frac{\partial \Phi}{\partial Z} - \varepsilon \omega \frac{\partial F}{\partial X} - \varepsilon \frac{\partial \Phi}{\partial X} \cdot$$

$$\left( \omega \frac{\partial^2 \Phi}{\partial X^2} - \varepsilon \frac{\partial F}{\partial X} \right) \sin^2 \theta - \varepsilon \frac{\partial \Phi}{\partial Y} \cdot$$

$$\left( \omega \frac{\partial^2 \Phi}{\partial X \partial Y} - \varepsilon \frac{\partial F}{\partial Y} \right) \cos^2 \theta \tag{21}$$

$$N_2[\eta, \Phi] = \eta - \omega \frac{\partial \Phi}{\partial X} + \varepsilon F \tag{22}$$

where

$$F = \frac{1}{2} \left[ \left( \frac{\partial \Phi}{\partial X} \sin \theta \right)^2 + \left( \frac{\partial \Phi}{\partial Y} \cos \theta \right)^2 + \left( \frac{\partial \Phi}{\partial Z} \right)^2 \right]$$

It is noted that the definitions for  $N_1[\cdot]$  and  $N_2[\cdot]$  are based on the two nonlinear boundary condition (12) and (11), respectively. When  $q$  increases from 0 to 1,  $\Phi$  and  $\eta$  vary continuously from their initial guess  $\phi_0$  and  $\zeta_0$  to the exact solutions  $\phi$  and  $\zeta$  of the original problems, respectively. The Taylor series for  $\Phi$  and  $\eta$  at  $q = 0$  are

$$\Phi = \phi_0 + \sum_{m=1}^{\infty} \phi_m q^m, \quad \eta = \zeta_0 + \sum_{m=1}^{\infty} \zeta_m q^m \tag{23}$$

where

$$\{\phi_m, \zeta_m\} = \frac{1}{m!} \frac{\partial^m}{\partial q^m} \{\Phi, \eta\} \Big|_{q=0}$$

Assuming that  $c_0$  is so properly chosen that the series in Eq.(23) converge at  $q = 1$ , we have the so-called homotopy-series solutions  $\phi = \Phi|_{q=1}$  and  $\zeta = \eta|_{q=1}$ . Furthermore, since the HAM provides extremely large freedom in the choice of auxiliary linear operators, we can only choose linear operators of  $\Phi$  in  $N_1[\cdot]$  as the auxiliary linear operator  $L_1[\cdot]$  by means of the solution expression (17) which is obtained under the physical considerations as

$$L_1[\Phi] = \omega_0^2 \frac{\partial^2 \Phi}{\partial X^2} + \frac{\partial \Phi}{\partial Z} \tag{24}$$

where  $\omega_0 = \sqrt{\tanh d}$  is the linear dispersion relation.

2.3 High-order deformation equations

The linear PDEs for the unknown  $\phi_m$  and  $\zeta_m$  can be derived directly from the zeroth-order deformation equations. Substituting the homotopy-Maclaurin series (23) into Eqs. (19)-(20), and equating the like-power of  $q$ , we have the so-called  $m$ th - order deformation equations

$$L_1[\phi_m] = c_0 \Delta_{m-1}^\phi + H_m S_{m-1} - \bar{S}_m \quad (Z = 0) \tag{25}$$

$$\zeta_m = c_0 \Delta_{m-1}^\zeta + H_m \zeta_{m-1} \quad (Z = 0) \tag{26}$$

where  $H_m = H(m - 2)$ , and  $H(\cdot)$  is the Heaviside step function. The explicit expression and detailed derivation for  $\Delta_{m-1}^\phi$ ,  $S_{m-1}$ ,  $\bar{S}_m$  and  $\Delta_{m-1}^\zeta$  are given in Appendix A.

One can see that the unknown terms  $\phi_m$  and  $\zeta_m$  are governed by linear PDEs (25) and (26). It should be noted that at this stage the sub-problems for  $\phi_m$  and  $\zeta_m$  are not only linear but also decoupled. Thus, these high-order deformation equations can easily be solved.

2.4 First-order approximation and dispersion relation

Substituting the initial guesses (18) and  $\zeta_0 = 0$  into Eq.(26), we can get

$$\zeta_1 = -c_0 A \left\{ \omega C \cos X \cos Y + \frac{\varepsilon A}{8} [1 + C^2 \cdot (1 - 2 \sin^2 \theta) \cos(2X) - (1 - C^2 + 2C^2 \sin^2 \theta) \cdot \cos(2Y) + (1 - C^2) \cos(2X) \cos(2Y)] \right\} \tag{27}$$

where  $C = \coth d$ . The coefficient  $\alpha_{0,1}$  in the initial approximation of  $\phi_0$  in Eq.(18) is still unknown. An additional equation which can be used to determine the value of  $A$  is

$$\zeta_1(0, e\pi) - \zeta_1(0, o\pi) = H \tag{28}$$

where  $e$  is an even integer,  $o$  an odd integer, and  $H$  the dimensionless wave height to first order based on the HAM. Then, using the inverse linear operator  $L_1$  in Eq.(25), we can get the solutions for  $A$  and  $\phi_1$  as follows

$$A = -\frac{H}{2c_0 \omega C} \tag{29}$$

$$\phi_1 = \sum_{i=1}^3 \sum_{j=0}^3 \alpha_{i,j} \sin(iX) \cos(jY) \cdot \cosh[\sqrt{(i \sin \theta)^2 + (j \cos \theta)^2} (Z + d)] \tag{30}$$

where  $\alpha_{i,j}$  is the  $(i, j)$ -th unknown coefficient.

We find the common solution  $\phi_1$  has one unknown coefficient  $\alpha_{1,1}$  which can be determined by avoiding the ‘‘secular’’ term  $\sin X$  in  $\phi_2$ . We note all subsequent functions occur recursively. By continuing the above approach, we can obtain higher-order functions  $\phi_m$  and  $\zeta_m$ . It should be mentioned that, based on the HAM, the dimensionless dispersion relation for nonlinear short-crested waves in a fluid of finite depth can be written as

$$\omega^2 - \frac{1}{\coth d} + \left( \frac{H\varepsilon}{8\omega c_0} \right)^2 [8 \sin^2 \theta (\sin^2 \theta - 1) + \frac{3}{\cosh^2 d}] = 0 \tag{31}$$

It is noted that the convergence control parameter  $c_0$  still retains in Eq.(31).

2.5 Optimal convergence-control parameter

Once we fix all parameters in the approximate series solutions, there is still an unknown convergence control parameter  $c_0$  which is used to guarantee the convergence of the series approximation. According to Liao<sup>[21]</sup>, the optimal value of  $c_0$  is determined by the minimum of the total squared residue  $\varepsilon_m^T$  for the nonlinear problem, which is defined by

$$\varepsilon_m^T + \varepsilon_m^\phi = \varepsilon_m^\zeta \tag{32}$$

where

$$\varepsilon_m^\phi = \frac{1}{(1 + M)^2} \sum_{i,j=0}^M \left[ \sum_{n=0}^m \Delta_n^\phi(i\Delta X, j\Delta Y) \right]^2,$$

$$\varepsilon_m^\zeta = \frac{1}{(1 + M)^2} \sum_{i,j=0}^M \left[ \sum_{n=0}^m \Delta_n^\zeta(i\Delta X, j\Delta Y) \right]^2$$

and  $\Delta_n^\phi$  and  $\Delta_n^\zeta$  are given in Appendix A,  $M$  is the number of the discrete points, and  $\Delta X = \pi/M$ . We choose  $M = 10$ . We can obtain the optimal  $c_0$  by the

minimum of  $\varepsilon_m^T$ .

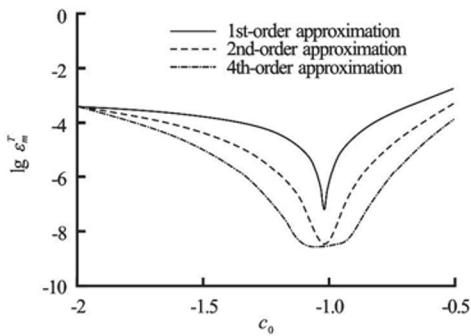


Fig.1 Residual squares of  $\lg \varepsilon_m^T$  versus  $c_0$

**Table 1** The total residual square error  $\varepsilon_m^T$  for different approximation order with  $m$  with  $c_0 = -1.0$

$m$	$\varepsilon_m^T$
2	$4.093 \times 10^{-9}$
4	$3.104 \times 10^{-9}$
6	$7.771 \times 10^{-10}$
8	$8.142 \times 10^{-11}$
10	$2.089 \times 10^{-12}$

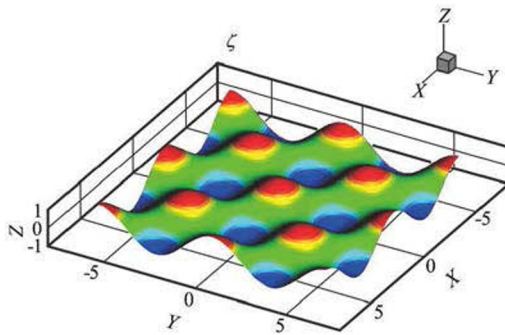
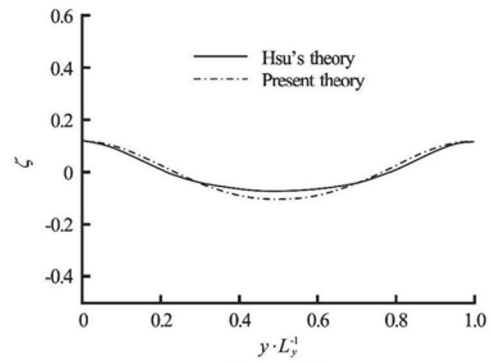


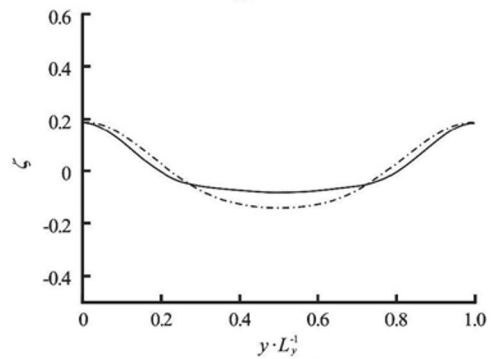
Fig.2 Wave profiles for  $d = 1.5\pi$ . The wave propagates in the  $X$  direction

### 3. Discussion and results

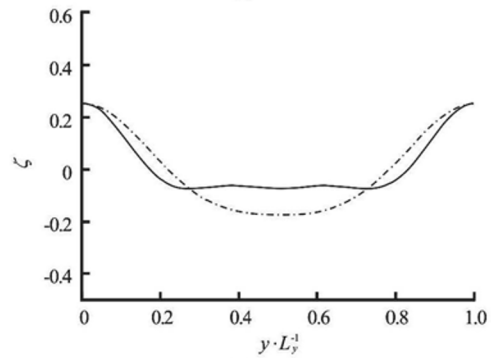
To choose an optimal value for the convergence control parameter  $c_0$  in such a way that all the series solutions for  $\phi$  and  $\zeta$  converge quickly, we firstly consider the case with  $d = 0.2\pi$ ,  $\varepsilon = 0.05$ ,  $\theta = \pi/4$ ,  $H = 0.15$  and take these data hereinafter for computation unless otherwise stated. The curves of the total residual square error  $\varepsilon_m^T$  at several orders versus the convergence-control parameter  $c_0$  are shown in Fig.1. We find that at every order  $\varepsilon_m^T$  has the smallest value



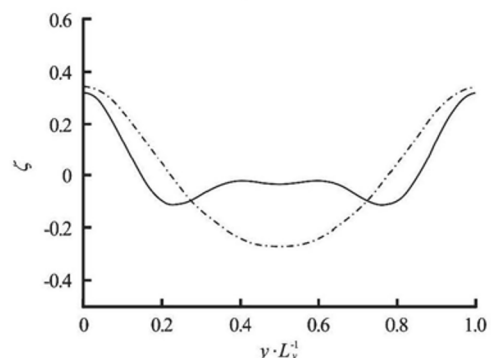
(a)  $\varepsilon = 0.10$



(b)  $\varepsilon = 0.15$



(c)  $\varepsilon = 0.20$



(d)  $\varepsilon = 0.25$

Fig.3 Comparison of our present dimensionless 3th-order surface profile  $\zeta$  with those of Hsu et al.<sup>[3]</sup> for different incident wave steepnesses  $\varepsilon$ .  $\theta = \pi/4$ ,  $d/L_y = 0.1$ ,  $t = 0$

which corresponds to the optimal  $c_0$ . For example, as

$m = 4$  and  $c_0 = -1.0$ , the smallest value of  $\varepsilon_4^T$  is  $3.104 \times 10^{-9}$ . So we choose  $c_0 = -1.0$ , and the total residual square error  $\varepsilon_m^T$  decreases quickly as the order  $m$  increases, as shown in Table 1. It is also found that  $\varepsilon_{10}^T$  can decrease to  $32.089 \times 10^{-12}$  at the 10th-order approximation, which indicates the convergence of the series solutions. It is demonstrated that the analytical solutions obtained here by means of the HAM are highly accurate. Figure 2 is the free surface profile for the short-crested waves, showing that the short-crested waves are periodic not only in the propagating direction but also in the perpendicular direction.

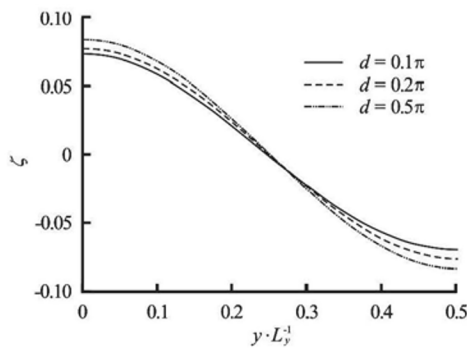


Fig.4 Wave profile  $\zeta$  versus  $y/L_y$  for different water depths  $d$

We compare the present solution for the wave profiles with that obtained by Hsu et al.<sup>[3]</sup> who used the perturbation techniques. Figure 3 is graphical representations for the 3rd-order solution in Eqs.(26) and (16) and the asymptotic solution in Eq.(70) in Ref.[3], in which  $\zeta$  is a function of  $y/L_y$  for different wave steepness  $\varepsilon$  and  $L_y$  is the wave length in the  $y$  direction. It can be seen from Fig.3 that the homotopy-series solution for the surface elevation at the crest near the wall  $y = 0$  is in good agreement with the perturbation-series approximation<sup>[3]</sup>, even in cases where  $\varepsilon$  is not small ( $\varepsilon > 0.2$ ). It is clear that the trough of surface elevation is steeper than those predicted by Hsu et al.<sup>[3]</sup>, especially in the cases with  $\varepsilon > 0.2$ . Thus the variations of the short-crested waves at the trough will be underestimated if the 3rd-order perturbation solution<sup>[3]</sup> is used for the wave deflection. We can also note that, as  $\varepsilon$  increases, the discrepancy between the two theories will become large for a finite  $\varepsilon$ , especially at the wave trough. The possible reason for this discrepancy is that the perturbation technology is strongly dependent on small physical parameters and then it usually breaks down as nonlinearity becomes strong (i.e.,  $\varepsilon$  increases), while the HAM is independent of any small parameters and thus it may be feasible for highly nonlinear problems.

Physical observation or experimental data are required in the future to verify the theoretical predictions.

Table 2  $K_E$  and  $P_E$  for Eqs.(13) and (14) with various water depths  $d$

$d$	$K_E$	$P_E$
$0.2\pi$	0.000496	0.000492
$0.5\pi$	0.000703	0.000705
$1.0\pi$	0.000705	0.000706
$1.5\pi$	0.000704	0.000707
$3.0\pi$	0.000704	0.000707

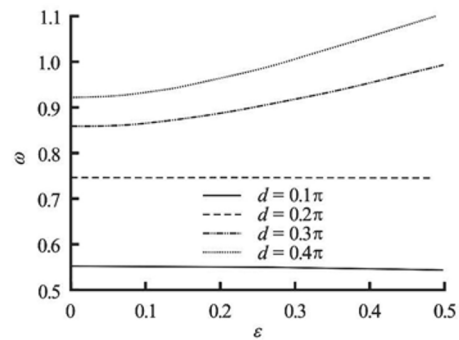


Fig.5 Angular frequency  $\omega$  versus the incident wave steepness  $\varepsilon$  for different water depths  $d$

The effect of the water depth  $d$  on the short-crested wave elevation  $\zeta$  is studied, as shown in Fig.4. We can see that the crest of wave elevation increases greatly with an increasing  $d$  and the steeper trough is formed. Most importantly, with a different viewpoint from all the research objectives in Refs.[1-7], we consider the effects of the water depth  $d$  on the mean kinetic energy density  $K_E$  and the mean potential energy density  $P_E$  of the nonlinear short-crested waves in detail. Different values of  $K_E$  and  $P_E$  for various water depths  $d$  are shown in Table 2. It is found that  $K_E$  and  $P_E$  are almost equal at every value of water depth  $d$ . A graphical representation for the nonlinear dispersion relation given by Eq.(31) with  $H = 1$  is shown in Fig.5. With the increase of incident wave amplitude  $\varepsilon$ , the angular frequency  $\omega$  increases for  $d < 0.2\pi$ , while for small  $d$ ,  $\omega$  decreases slightly as  $\varepsilon$  increases from 0 to 0.5. We can also find that the angular frequency  $\omega$  becomes large with the increment of the water depth. Figure 6 shows the kinetic energy density  $P_E$  of short-crested waves for different angles of incidence  $\theta$  in various water depths. It can be seen from Fig.6 that the short-crested waves

with the larger  $\theta$  always contain larger  $P_E$  in different water depths. Figure 7 illustrates the variation of the dimensionless wave pressure  $p$  acting on the vertical wall as a function of  $X$  for different small parameter  $\varepsilon$ . It can be seen from Fig.7 that, as  $\varepsilon$  increases, the crests and the troughs of the pressure  $p$  in the 3rd-order approximation become steeper and steeper.

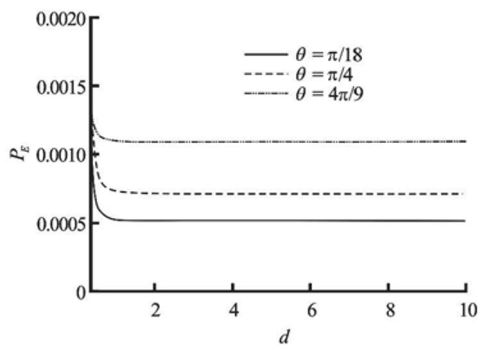


Fig.6 Kinetic energy density  $P_E$  versus the water depth  $d$  for different incident angles  $\theta$

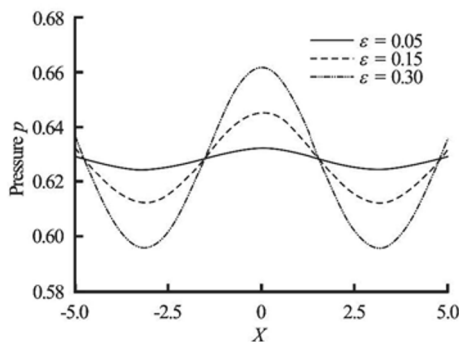


Fig.7 Wave pressure  $p$  versus  $X$  for different  $\varepsilon$

#### 4. Conclusions

A system of nonlinear short-crested waves in a fluid of finite depth is studied analytically using the homotopy analysis method. Instead of solving the nonlinear PDEs for the waves directly by means of other analytical techniques, we reconstruct a new family of nonlinear PDEs as the zeroth-order deformation equations. Then the nonlinear PDEs are further transferred into an infinite number of linear PDEs, namely the higher-order deformation equations on the known boundary, which can easily be solved. More importantly, the highly convergent series solutions for the fully nonlinear wave equations are obtained by choosing the optimal convergence control parameter. Besides, the homotopy-series approximations showing the behavior of nonlinear short-crested waves are compared with the previously reported asymptotic solutions, and the agreement

is very good for weakly nonlinear waves especially at the wave crest. These conclusions demonstrate the accuracy and validity of the HAM for the nonlinear short-crested wave problems.

The homotopy-based dispersion relation shows that the wave frequency of short-crested wave system is affected by incident wave steepness and water depth. The frequency  $\omega$  becomes large with the increment of the water depth. Incident wave steepness also causes analogous influence on the frequency except that water depth  $d$  ( $d < 0.2\pi$ ) is small.

The effects of the water depth and the incidence angle on the wave energy including the kinetic and the potential energies for nonlinear short-crested waves are analyzed detailedly. At every value of water depth, the values of the kinetic and the potential energies are nearly equal. A particularly interesting feature of the results here is that, in various water depths, the larger incidence angles is, the more potential energy is. Furthermore, we study the influence of the water depth on the wave elevation and the effect of incident wave steepness on the wave pressure. It is found that, as the water depth increases, the wave elevation is smoothed at the crest and is sharpen at the trough. And the wave pressure exerted on the vertical wall will become larger with the increasing wave steepness. All these results demonstrate that the angle of incidence, the water depth and incident wave steepness have important effects on the energy, the pressure and the profile of nonlinear short-crested waves in a fluid of finite depth.

#### Acknowledgement

The authors thank the anonymous reviewers for their constructive comments.

#### References

- [1] FUCHS R. A. **On the theory of short-crested oscillatory waves**[M]. Washington, USA: U.S. National Bureau Standards, 1952, 521: 187-200.
- [2] CHAPPELEAR J. E. **On the description of short-crested wave**[M]. Washington, USA: US Beach Erosion Board, 1961, 125.
- [3] HSU J. R. C., TSUCHIYA Y. and SILVESTER R. Third-order approximation to short-crested waves[J]. **Journal of Fluid Mechanics**, 1979, 90: 179-196.
- [4] ROBERTS A. J. Nonlinear buoyancy effects in fluids[D]. Doctoral Thesis, Cambridge, UK: University of Cambridge, 1982.
- [5] FENTON J. D. Wave forces on vertical walls[J]. **Journal of Waterway, Port, Coastal, and Ocean Engineering**, 1985, 111(4): 693- 718.
- [6] JIAN Y. J., ZHU Q. Y. and ZHANG Z. J. et al. Third order approximation to capillary gravity short crested waves with uniform currents[J]. **Applied Mathematical Modelling**, 2009, 33: 2035-2053.

- [7] ROBERTS A. J. Highly nonlinear short-crested water waves[J]. **Journal of Fluid Mechanics**, 1983, 135: 301-321.
- [8] LIAO Shi-jun. The proposed homotopy analysis technique for the solution of nonlinear problems[D]. Doctoral Thesis. Shanghai, China: Shanghai Jiao Tong University, 1992(in Chinese).
- [9] VASAN V., DECONINCK B. The Bernoulli boundary condition for traveling water waves[J]. **Applied Mathematics Letters**, 2013, 26: 515-519.
- [10] LIAO S., CAMPO A. Analytic solutions of the temperature distribution in Blasius viscous flow problems[J]. **Journal of Fluid Mechanics**, 2002, 453: 411-425.
- [11] LIAO S. An optimal homotopy-analysis approach for strongly nonlinear differential equations[J]. **Communications in Nonlinear Science and Numerical Simulation**, 2010, 15(8): 2003-2016.
- [12] CHENG J., ZHU S. and LIAO S. An explicit series approximation to the optimal exercise boundary of American put options[J]. **Communications in Nonlinear Science and Numerical Simulation**, 2010, 15(5): 1148-1158.
- [13] CHENG Jun, DAI Shi-qiang. A uniformly valid series solution to the unsteady stagnation-point flow towards an impulsively stretching surface[J]. **Science China Physics, Mechanics and Astronomy**, 2010, 53(3): 521-526.
- [14] CANG Jie, CHENG Jun and GRIMSHAW Roger. Short comment on the effect of a shear layer on nonlinear water waves[J]. **Science China Physics, Mechanics and Astronomy**, 2011, 54(1): 67-73.
- [15] LIAO S., CHEUNG K. F. Homotopy analysis of nonlinear progressive waves in deep water[J]. **Journal of Engineering Mathematics**, 2003, 45(2): 105-116.
- [16] TAO L., SONG H. and CHAKRABARTI S. Nonlinear progressive waves in water of finite depth - an analytic approximation[J]. **Coastal Engineering**, 2007, 54(11): 825-834.
- [17] LIAO S. On the homotopy multiple-variable method and its applications in the interactions of nonlinear gravity waves[J]. **Communications in Nonlinear Science and Numerical Simulation**, 2011, 16(3): 1274-1303.
- [18] XU D., LIN Z. and LIAO S. et al. On the steady-state fully resonant progressive waves in water of finite depth[J]. **Journal of Fluid Mechanics**, 2012, 710: 379-418.
- [19] WANG Ping, LU Dong-qiang. Analytic approximation to nonlinear hydroelastic waves traveling in a thin elastic plate floating on a fluid[J]. **Science China Physics, Mechanics and Astronomy**, 2013, 56(11): 2170-2177.
- [20] LIAO S. **Beyond perturbation: Introduction to the homotopy analysis method**[M]. Boca Raton, USA: CRC Press, 2004.
- [21] LIAO Shi-jun. **Homotopy analysis method in nonlinear differential equations**[M]. Beijing, China: Higher Education Press, 2012.

**Appendix A: The detailed derivation of the Eqs.(25) and (26) and the expression for  $\phi_m$  and  $\zeta_m$**

$$\eta^n = \left( \sum_{i=1}^{\infty} \zeta_i q^i \right)^n = \sum_{i=n}^{\infty} \mu_{n,i} q^i \quad (A1)$$

For any  $Z$ , we have a Maclaurim series

$$\phi_m = \sum_{n=0}^{\infty} \frac{1}{n!} \frac{\partial^n \phi_m}{\partial Z^n} \Big|_{Z=0} Z^n \quad (A2)$$

For  $Z=\eta$ , it follows from Eqs.(A1) and (A2) that

$$\phi_m = \sum_{n=0}^{\infty} \frac{1}{n!} \frac{\partial^n \phi_m}{\partial Z^n} \Big|_{Z=0} \left( \sum_{i=n}^{\infty} \mu_{n,i} q^i \right) = \sum_{i=0}^{\infty} \psi_{m,i} q^i \quad (A3)$$

where

$$\psi_{m,i} = \sum_{n=0}^i \left( \frac{1}{n!} \frac{\partial^n \phi_m}{\partial Z^n} \Big|_{Z=0} \right) \mu_{n,i}$$

Thus we have, for  $Z = \eta$

$$\Phi = \sum_{m=0}^{\infty} \phi_m q^m = \sum_{m=0}^{\infty} \varphi_m q^m \quad (A4)$$

where

$$\varphi_m = \sum_{i=0}^m \psi_{m-i,i}$$

Substituting the series expansions (A1) and (A4) into the boundary conditions (19) and (20), then equating the like-power of the embedding parameter  $q$ , we have two linear boundary conditions (25) and (26) respectively. The explicit expressions for  $\Delta_{m-1}^{\phi}$ ,  $S_{m-1}$ ,  $\bar{S}_m$  and  $\Delta_{m-1}^{\zeta}$  in these two conditions are given by

$$\Delta_{m-1}^{\phi} = \omega^2 \frac{d^2 \varphi_{m-1}}{dX^2} + \bar{\varphi}_{m-1} - \omega \varepsilon \bar{f}_{m-1,1} - \varepsilon S^2 \cdot$$

$$\sum_{n=0}^{m-1} \frac{\partial \varphi_n}{\partial Y} \left( \omega \frac{\partial^2 \varphi_{m-1-n}}{\partial X^2} - \varepsilon \bar{f}_{m-1-n,1} \right) - \varepsilon (1 - S^2) \cdot$$

$$\sum_{n=0}^{m-1} \frac{\partial \varphi_n}{\partial Y} \left( \omega \frac{\partial^2 \varphi_{m-1-n}}{\partial X \partial Y} - \varepsilon \bar{f}_{m-1-n,2} \right) \quad (m \geq 1) \quad (A5)$$

$$S_{m-1} = \sum_{i=0}^{m-1} \left( \frac{1}{C} \frac{\partial^2 \psi_{m-1-i,i}}{\partial X^2} + \gamma_{m-1-i,i} \right) \quad (m \geq 1) \quad (A6)$$

$$\bar{S}_m = \sum_{i=1}^m \left( \frac{1}{C} \frac{\partial^2 \psi_{m-i,i}}{\partial X^2} + \gamma_{m-i,i} \right) \quad (A7)$$

$$\Delta_{m-1}^{\zeta} = \frac{1}{2} \varepsilon \sum_{n=0}^{m-1} \left[ \frac{\partial \varphi_n}{\partial X} \frac{\partial \varphi_{m-1-n}}{\partial X} S^2 + \frac{\partial \varphi_n}{\partial Y} \frac{\partial \varphi_{m-1-n}}{\partial Y} \right. \\ \left. (1-S^2) + \bar{\varphi}_n \bar{\varphi}_{m-1-n} \right] + \zeta_{m-1} - \omega \frac{\partial \varphi_{m-1}}{\partial X} \quad (m \geq 1) \quad (\text{A8})$$

where

$$S = \sin \theta, \quad \bar{\varphi}_m = \sum_{i=0}^m \gamma_{m-i,i},$$

$$\gamma_{m-i,i} = \sum_{n=0}^i \frac{1}{n!} \left( \frac{\partial^{n+1} \phi_{m-i}}{\partial z^{n+1}} \Big|_{z=0} \right) \mu_{n,i},$$

$$\bar{f}_{m,1} = \sum_{n=0}^m \left[ \frac{\partial \varphi_n}{\partial X} \frac{\partial^2 \varphi_{m-n}}{\partial X^2} S^2 + \frac{\partial \varphi_n}{\partial Y} \frac{\partial^2 \varphi_{m-n}}{\partial X \partial Y} (1-S^2) + \bar{\varphi}_n \frac{\partial \bar{\varphi}_{m-n}}{\partial X} \right],$$

$$\bar{f}_{m,2} = \sum_{n=0}^m \left[ \frac{\partial \varphi_n}{\partial X} \frac{\partial^2 \varphi_{m-n}}{\partial X \partial Y} S^2 + \frac{\partial \varphi_n}{\partial Y} \frac{\partial^2 \varphi_{m-n}}{\partial Y^2} (1-S^2) + \bar{\varphi}_n \frac{\partial \bar{\varphi}_{m-n}}{\partial Y} \right]$$

## Appendix B: Expressions of the coefficients

$$\alpha_{1,0} = \alpha_{1,2} = \alpha_{2,1} = \alpha_{2,3} = \alpha_{3,0} = \alpha_{3,2} = 0 \quad (\text{B1})$$

$$\alpha_{1,1} = c_1 \{c_2 [S_9 (c_3 C_8 + c_4 S_8) + C_9 + c_5 C_8 + c_6 S_8] + c_7 \cosh(2dS) + c_8 \sinh(2dS)\} \quad (\text{B2})$$

$$\alpha_{1,3} = H^3 \varepsilon^2 [-3 + 3C^2 + 4(1-2C^2)S^2 + 4C^2 S^4] \cdot [128\omega^3 C c_0^2 (C S_9 \sqrt{9-8S^2} - C_9)]^{-1} \quad (\text{B3})$$

$$\alpha_{2,0} = H^2 \varepsilon (-1 - 2C^2 + 4C^2 S^2) \{32\omega C c_0 \cdot [CS \sinh(2dS) - 2 \cosh(2dS)]\}^{-1} \quad (\text{B4})$$

$$\alpha_{2,2} = H^2 \varepsilon (-1 + 2C^2) \{32\omega C c_0 [C \sinh(2d) - 2 \cosh(2d)]\}^{-1} \quad (\text{B5})$$

$$\alpha_{3,1} = H^3 \varepsilon^2 (1 - C^2 - 4S^2 + 4C^2 S^4) \cdot [128\omega^3 C c_0^2 (C \sqrt{1+8S^2} S_8 - 9C_8)]^{-1} \quad (\text{B6})$$

$$\alpha_{3,3} = H^3 \varepsilon^2 (-1 + C^2) \{384\omega^3 C c_0^2 [C \sinh(3d) - 3 \cosh(3d)]\}^{-1} \quad (\text{B7})$$

where

$$S_8 = \sinh(d\sqrt{1+8S^2}), \quad C_8 = \cosh(d\sqrt{1+8S^2}),$$

$$S_9 = \sinh(d\sqrt{9-8S^2}), \quad C_9 = \cosh(d\sqrt{9-8S^2}),$$

$$c_1 = C^3 H^3 \varepsilon^2 \{1024D\omega^3 c_0^2 \{3H^2 [-3 - 4C^2 + C^4 (7 - 16S^2 + 16S^4)] \varepsilon^2 + 128C^3 \omega^2 (-1 + C\omega^2) c_0^2\}\}^{-1},$$

$$c_2 = [C^5 (C_9 - C S_9 \sqrt{9-8S^2}) (-9C_8 + C S_8 \sqrt{1+8S^2})]^{-1},$$

$$c_3 = H^2 \varepsilon^2 C (-1 + C^2)^4 \sqrt{9-8S^2} [45 + 32D^8 S^2 \cdot (29 - 43S^2 + 8S^4 + 6S^6) + 64D^6 (-35 + 80S^2 - 58S^4 + 22S^6 + 18S^8) + 32D^4 (-39 + 68S^2 - 43S^4 + 56S^6 + 48S^8) + 2D^2 (199 - 576S^2 + 480S^4 + 320S^6 + 288S^8)],$$

$$c_4 = H^2 \varepsilon^2 C^2 \sqrt{9+64S^2 - 64S^4} [-47 - 18C^6 - 5C^8 - 2C^2 (63 - 32S^2 + 32S^4) + 4C^4 (49 - 176S^2 + 176S^4)],$$

$$c_5 = -H^2 \varepsilon^2 [-9 + 45C^8 + 2C^2 (959 - 2176S^2 + 128S^4) + 4C^4 (-2973 + 9200S^2 - 8752S^4 + 2048S^6) + C^6 (9938 - 42560S^2 + 61504S^4 - 34816S^6 + 7680S^8)],$$

$$c_6 = H^2 \varepsilon^2 C \sqrt{1+8S^2} [-25 + 5C^8 + 96S^2 + 2C^2 (99 - 176S^2 + 144S^4) + 4C^4 (-319 + 1016S^2 - 992S^4 +$$

$$224S^6) + 2C^6(549 - 2352S^2 + 3440S^4 - 1984S^6 + 384S^8),$$

$$c_7 = 512\omega^4 \{16S^2[-1 + C^2(-2 + 4S^2)] + 8(-1 + C^2)^2(2 + 5D^2 + 2D^4)\} \{C[2 \cosh(2dS) - S \sinh(2dS)]\}^{-1},$$

$$c_8 = 2048\omega^4 S(-1 + C^2)^2(2 + 5D^2 + 2D^4) \cdot [2 \cosh(2dS) - S \sinh(2dS)]^{-1},$$

$$D = \sinh d$$